Title
Mosquito cryptochromes expressed in Drosophila confer species-specific behavioral light responses.

Journal
Current Biology, 32(17)

Authors
Au, David
Foden, Alexander
Park, Soo
et al.

Publication Date
2022-09-12

DOI
10.1016/j.cub.2022.07.021

Peer reviewed

HHS Public Access

Author manuscript

Curr Biol. Author manuscript; available in PMC 2023 September 12.

Published in final edited form as:

Curr Biol. 2022 September 12; 32(17): 3731–3744.e4. doi:10.1016/j.cub.2022.07.021.

Mosquito Cryptochromes expressed in *Drosophila* confer species-specific behavioral light responses

David D. Au[1], **Alexander J. Foden**[1], **Soo Jee Park**[1], **Thanh H. Nguyen**[1], **Jenny C. Liu**[1], **Mary D. Tran**[1], **Olga G. Jaime**[1], **Zhaoxia Yu**[2,3], **Todd C. Holmes**[1,3,4,*]

[1]Department of Physiology and Biophysics, School of Medicine, University of California, Irvine, Irvine, CA 92697, USA

[2]Department of Statistics, Donald Bren School of Information and Computer Sciences, University of California, Irvine, Irvine, CA 92697, USA

[3]Center for Neural Circuit Mapping, University of California, Irvine, CA 92697, USA

[4]Lead Contact

Summary

CRYPTOCHROME (CRY) is a short-wavelength light-sensitive photoreceptor expressed in a subset of circadian neurons and eyes in *Drosophila* that regulates light evoked circadian clock resetting. Acutely, light evokes rapid electrical excitation of the ventral lateral subset of circadian neurons and confers circadian modulated avoidance behavioral responses to short wavelength light. Recent work shows dramatically different avoidance versus attraction behavioral responses to short wavelength light in day-active versus night-active mosquitoes; and that these behavioral responses are attenuated by CRY protein degradation by constant light exposure in mosquitoes. To determine whether CRY1s mediate species-specific coding for behavioral and electrophysiological light-responses, we used an “empty neuron” approach and transgenically expressed diurnal *Aedes aegypti* (AeCRY1) versus nocturnal *Anopheles gambiae* (AgCRY1) in a *cry-null Drosophila* background. AeCRY1 is much less light sensitive than either AgCRY1 or DmCRY as shown by partial behavioral rhythmicity following constant light exposure. Remarkably, expression of nocturnal AgCRY1 confers low survival to constant white light as does expression of AeCRY1 to a lesser extent. AgCRY1 mediates significantly stronger electrophysiological cell autonomous responses to 365 nm ultraviolet (UV) light relative to AeCRY1. AgCRY1 expression mediates electrophysiological and behavioral sensitivity to 635 nm red light while AeCRY1 does not, consistent with species-specific mosquito red light responses. AgCRY1 and DmCRY mediate

[*]**Correspondence** tholmes@uci.edu.

Author Contributions

Conceptualization, D.D.A. and T.C.H.; Methodology, D.D.A. and T.C.H.; Software, D.D.A.; Formal Analysis, D.D.A., A.J.F., S.P., T.H.N., J.C.L., M.D.T., and Z.Y.; Investigation, D.D.A., A.J.F., S.P., T.H.N., J.C.L., and M.D.T.; Writing – Original Draft, D.D.A. and T.C.H.; Writing – Review & Editing, D.D.A., Z.Y., and T.C.H.; Funding Acquisition, D.D.A. and T.C.H.; Resources, Z.Y. and T.C.H.; Supervision, T.C.H

Declaration of Interests

The authors have no financial interests to declare.

intensity-dependent avoidance behavior to UV light at different light intensity thresholds, while AeCRY1 does not, thus mimicking mosquito and fly behaviors. These findings highlight CRY as a key non-image forming visual photoreceptor that mediates physiological and behavioral light-responses in a species-specific fashion.

eToc Blurb

Au et al. show that transgenic expression of diurnal and nocturnal mosquito species' CRY in *Drosophila* transduce light-evoked behavior and neurophysiological effects matching their functions in mosquitoes. Nocturnal mosquito CRY1 shows significantly greater behavioral and electrophysiological light responses than diurnal mosquito CRY1.

Introduction

Mosquitoes are lethal disease vectors that account for hundreds of millions of infections and millions of human deaths each year[1]. Female mosquitoes seeking blood meals for reproductive energy hunt using an arsenal of finely tuned sensors for smell, taste, temperature, and sight[2–7]. The predominant current mosquito control strategies use environmentally damaging toxic pesticides[8–10]. Short-wavelength light (UV, violet, blue) evokes diverse behaviors in insects, including arousal, phototaxis/photoavoidance, circadian entrainment, and others[11–17]. Until recently, it was widely assumed that all behavioral responses to short wavelength light are mediated by opsin-based image forming photoreception in insect eyes[14,16,18,19]. However, many light-regulated behaviors have been found recently to be regulated by the non-opsin photoreceptor CRYPTOCHROME (CRY)[12,20–22]. CRY is a light-sensing flavin-based photopigment that detects UV and blue light in its FAD oxidized and FAD•- anionic semiquinone semi-reduced states and red light in its FADH• neutral radical state[23–27]. *Drosophila* CRY is expressed in a small number of central brain arousal and circadian neurons and external photoreceptors[22,28–31]. In contrast to the rapid on/off electrophysiological light responses mediated by image forming opsins, CRY photoactivation evokes rapid and very long-lasting (30–40 sec) neuronal depolarization and increased action potential firing in large ventral lateral neurons (l-LNvs)[11,20–22]. LNv CRY phototransduction mediates UV light avoidance behavior in flies[11,21,32]. Recent findings show *An. gambiae* mosquitoes are behaviorally photophobic to UV light, while *Ae. aegypti* mosquitoes exhibit phototaxis to UV light[33]. We hypothesize that mosquito species-specific light response behaviors are mediated by species-specific CRY isoforms, considering that light intensity, spectral composition, circadian timing, and different light input channels may also contribute to light-modulated behaviors. We are interested in understanding the basis for these poorly understood light response behaviors for better control of harmful disease-spreading insects.

Results

AeCRY1 and AgCRY1 expression does not determine diurnal/nocturnal behavior or the time-of-day peak of the circadian clock in transgenic flies

Drosophila CRY (DmCRY) mediates light-induced degradation of TIM, thus resetting the circadian clock and rhythms in flies[29,34]. Diurnal *Ae. aegypti* mosquitoes and nocturnal

An. gambiae mosquitoes show opposite phases of sleep/wake activity cycles and 12 hr differences in their circadian clock peak phase[33]. To determine whether CRY expression of day versus night active mosquitoes is sufficient to set the circadian clock to peak time, we employ an established "empty neuron system" approach for interspecific transformation for studying species-specific effects[35–39]. The l-LNvs do not drive circadian behavior on their own as shown by mosaic analysis[35]. We tested the effects of mosquito AeCRY1 and AgCRY1 expression in *Drosophila* by generating transgenic UAS-flies to express CRY1 over a *cry-null* mutant fly background from *Ae. aegypti* (AeCRY1) or *An. gambiae* (AgCRY1) using the *crypGAL4–24* driver to express in all cells that ordinarily express CRY[36]. The amino acid sequence comparison of DmCRY (positive control), AgCRY1 and AeCRY1 is shown in Figure S1. The N-terminal fusion of eGFP verifies protein expression levels and shows all three CRYs with levels of expression less than an order of magnitude difference (Figure S2). To test whether mosquito CRY1s determine the circadian clock peak, TIM levels were measured at time points ZT5, ZT11, ZT17, and ZT23 in the lateral ventral neuron (LNv) subgroup after at least three days of 12:12 hr Light:Dark (LD) entrainment, and show peak signal at ZT23 and lowest signal at ZT5 and ZT11 for control DmCRY, AeCRY1, and AgCRY1 expressing transgenic flies (Figure 1A, B, C, D, E, F, G). AeCRY1 TIM values are almost two times higher than AgCRY1 flies, suggesting that AeCRY1 from the day-active mosquito is less light sensitive than nocturnal AgCRY1. Negative control *cry-null* flies lacking CRY expression show a similar pattern of TIM cycling in the LNvs (Figure 1H). CRY variant and TIM expression in the number of LNvs in the brain is shown in Figure S3. Thus, AeCRY1 and AgCRY1 expression in flies does not disrupt the circadian clock or determine the timing of the TIM peak.

AgCRY1 expressing flies show greater intensity-dependent light sensitivity than AeCRY1 expressing flies based on their comparative degree of arrhythmicity in an LL assay

Constant light (LL) evokes behavioral arrhythmicity while flies lacking functional CRY maintain greater rhythmicity under LL[20,37]. To determine the relative light sensitivities of mosquito CRY1s, we tested locomotor rhythmicity after subjecting transgenic and *cry-null* control flies to at least five days of intensity-tuned 12:12 hr LD entrainment, followed by at least five days of LL white light at high (1000 lux) or low (1 lux) intensity. DmCRY expressing flies become highly arrhythmic in high intensity LL (Figure 2A) and negative control *cry-null* flies maintain a high level of rhythmicity in all LL light conditions, confirming the absence of functional CRY (Figure 2D, Figure 3D). AeCRY1 expressing flies are partially arrhythmic in high and low intensity LL, showing higher rhythmicity than DmCRY expressing flies, but significantly less rhythmicity than *cry-null* flies, suggesting AeCRY1 is functional but less light sensitive by this measure (Figure 2B, Figure 3B). AgCRY1 flies exhibit significantly less rhythmicity in high intensity LL relative to AeCRY1 flies, showing greater light sensitivity of AgCRY1 compared to AeCRY1 (Figure 2C, E). AgCRY1 expressing flies exhibit arrhythmicity in response to high intensity LL that is indistinguishable to DmCRY expressing flies (Figure 2E), but maintain detectable rhythmicity in low intensity LL (Figure 3C).

Unexpectedly, both AgCRY1 and AeCRY1 flies die in progressively greater numbers when exposed to prolonged high intensity 1000 lux white light LL compared to DmCRY and

cry-null groups. AgCRY1 show the highest mortality after seven days of LL (Figures 2F–H). At low intensity 1 lux LL, AgCRY1 and AeCRY1 flies also exhibit higher mortality after prolonged LL exposure (Figures 3F–H). AgCRY1 flies exhibit significantly higher mortality in 1000 lux LL at day 7 relative to 1 lux LL at day 7, showing that LL mortality is a function of light intensity (Figure 2H, Figure 3H). This phenomenon may be related to CRY mediated modulation of lifespan in aged flies[38]. Diurnal AeCRY1 expressing flies are less light sensitive than nocturnal AgCRY1 expressing flies by the LL mortality assay. Thus the relative light sensitivities of mosquito CRY1s may contribute to the very strong light avoidance seen in nocturnal mosquitoes[33].

AgCRY1 mediates more robust cell autonomous electrophysiological responses to short-wavelength and red light than AeCRY1

Drosophila LNvs are circadian/arousal neurons that drive CRY-dependent photoavoidance[12,17,20,21,32]. As nocturnal mosquitoes exhibit strong short wavelength photoavoidance[33], we tested the hypothesis that nocturnal mosquito AgCRY1 confers cell autonomous greater electrophysiological responsiveness to 365 nm UV light than diurnal AeCRY1. We expressed AeCRY1, AgCRY1, and control DmCRY in the *cry-null* genetic background flies using the *pdfGAL4* driver line to restrict expression to the LNvs, then compared electrophysiological responses to 365 nm UV light over a four order of magnitude intensity range (200 μW/cm^2, 20 μW/cm^2, 2 μW/cm^2 and 0.2 μW/cm^2) measured by whole-cell patch-clamp recordings of l-LNvs in transgenic flies. *Drosophila* eye and head cuticles are >85% and 50% transparent respectively to 365 nm UV light[22]. DmCRY expressing l-LNvs show robust light evoked increases in firing frequency (FF) at 200, 20, 2 and 0.2 μW/cm^2 light intensities (Figure 4A). AgCRY1 UV light evoked FF increases are significantly higher than stimulus intensity matched AeCRY1 UV light evoked FFs at 200 μW/cm^2, 2 μW/cm^2, and 0.2 μW/cm^2 (Figure 4A), thus AgCRY1 consistently exhibits higher electrophysiological light sensitivity relative to AeCRY1. While DmCRY UV light evoked FFs are higher than either mosquito CRY1, comparing the absolute performances of native versus heterologously expressed CRY proteins is interpretationally questionable[27,39,40]. Representative l-LNv patch clamp voltage traces depicting 1-minute raw action potential firing data in response to 365 nm UV light stimulus at 200 μW/cm^2 are shown in Figure S5.

The relationship between light onset and the timing of the first light evoked action potential is not kinetically robust[22]. We developed a kinetically robust CRY mediated light evoked potential method[20,22] using signal averaging of multiple current-clamp recordings. Control DmCRY light evoked responses increase sharply during and immediately after the UV light pulse for all four UV light intensities tested (200 μW/cm^2, 20 μW/cm^2, 2 μW/cm^2, and 0.2 μW/cm^2), followed by intensity-dependent monotonically decreasing levels of sustained responses over tens of seconds post light stimulus (Figure 4B, D, F, and H). In contrast, very weak or absent UV light responses are seen for evoked potential recordings from *cry-nulls* at all light intensities tested (Figure 4B, D, F, and H) that are significantly less than DmCRY, particularly during and several seconds after the 5 sec 200 μW/cm^2 UV light pulse (Figure 4B).

AgCRY1 mediates remarkably sustained evoked potentials in response to the 200 μW/cm^2 365 nm UV light stimulus, as seen up to 45 seconds after the cessation of the UV light pulse (Figure 4C). 200 μW/cm^2 UV light evoked AgCRY1 potentials show significantly higher magnitude evoked increases in membrane potential than AeCRY1 at nearly all time points after the light pulse, statistically calculated using FDR adjustment for which $p \leq 0.1$ indicates significance (Figure 4C). The 200 μW/cm^2 UV light evoked AeCRY1 potential after the cessation of light is sustained, but significantly less than that for AgCRY1. Similar results are seen for all lower stimulus intensities: AgCRY1 UV light evoked responses tend to be significantly higher than AeCRY1 recorded following 20 μW/cm^2, 2 μW/cm^2, and 0.2 μW/cm^2 365 nm UV light stimulus (Figure 4E, G and I). Thus, cell autonomous AgCRY1 UV light evoked responses are significantly higher than those of AeCRY1 over a wide range of light intensities. These results indicate that the greater light response of AgCRY1 over AeCRY1 is likely due to intrinsic CRY molecular properties.

The LNv/circadian neural circuit networks in nocturnal *Anopheles coluzzi* and diurnal *Aedes* mosquitoes show similar and species specific features and share neuroanatomical features with *Drosophila*[33]. To determine whether circuit-wide expression of mosquito CRY1s confer distinguishable electrophysiological differences compared to expression restricted to the LNvs, we used the *crypGAL4–24* driver line that drives expression in all CRY neurons. DmCRY expression via the *crypGAL4–24* driver mediates robust electrophysiological light responses in the l-LNvs that do not differ from endogenous wild type CRY (Figure S4). DmCRY expression driven by the *crypGAL4–24* driver mediates robust and significant increases in FF in the l-LNvs in response to 200 μW/cm^2 UV light relative to *cry-null* (blue column, Figure 5A). DmCRY expression restricted to LNvs also mediates robust and significant increases in FF in the l-LNvs in response to 200 μW/cm^2 UV light relative to *cry-null* (light blue column, Figure 5A). AeCRY1 expression restricted to LNvs mediates little or no change in firing in response to 200 μW/cm^2 UV light (light orange column, Figure 5A) and appears nearly identical to the lack of light response under these conditions to *cry-null* (grey column, Figure 5A). Light responses from *crypGAL4–24* driven DmCRY, AeCRY1, and AgCRY1 are significantly greater than *pdfGAL4* driven AeCRY1 (Figure 5A). AeCRY1 expressed in all CRY neurons, however, does show a significant light evoked response compared to *cry-null* in response to 200 μW/cm^2 UV light (orange column, Figure 5A), perhaps due to a compounding effect of CRY1 photoactivation in other clock neurons. In contrast, AgCRY1 expression restricted to LNvs mediates significant increases in firing in response to 200 μW/cm^2 UV light (light purple column, Figure 5A) relative to *cry-null*, but significantly less than the 200 μW/cm^2 UV light response measured from transgenics that express DmCRY and AgCRY1 driven in all CRY expressing neurons (blue and purple columns, respectively, Figure 5A). Comparing the FF ratio during stimulus and several 10-second bins post-stimulus along with their evoked potential profiles (Figure 5E, F, G), *crypGAL4–24* driven DmCRY and *pdfGAL4* driven AgCRY1 show a sustained response to UV light (Figure 5B, D, E, G), whereas *pdfGAL4* driven DmCRY, *pdfGAL4* and *crypGAL4–24* driven AeCRY1, and *crypGAL4–24* driven AgCRY1 rapidly return to baseline after stimulus (Figure 5C, D, F). The FF ratio for *crypGAL4–24* driven DmCRY is significantly higher than *pdfGAL4* driven DmCRY and *cry-null* up to the 10 second post-stimulus bin (Figure 5B). *crypGAL4–24* driven AeCRY1

UV light evoked FF is significantly higher than *pdfGAL4* driven AeCRY1 UV light evoked FF during stimulus and at the 30 second post-stimulus bin, but after FDR adjustment, only shows significance during stimulus (Figure 5C). Both *crypGAL4–24* driven AgCRY1 UV light evoked FF and *pdfGAL4* driven AgCRY1 UV light evoked FF are significantly greater than *cry-null* but not relative to each other (Figure 5D).

Recordings from l-LNvs expressing DmCRY using the *pdfGAL4* or *crypGAL4–24* driver show significantly greater UV light evoked potentials relative to the *cry-null* negative control. The *pdfGAL4* driven DmCRY membrane potential response rapidly returns to baseline after stimulus, while the *crypGAL4–24* driven DmCRY response sustains for approximately 30–40 seconds post-stimulus and remains significant compared to the *cry-null* and the *pdfGAL4* driven DmCRY responses (Figure 5E). Both the *pdfGAL4* and *crypGAL4–24* driven AeCRY1 membrane potential UV light responses rapidly return to baseline, but the *crypGAL4–24* driven AeCRY1 shows a greater and slightly more sustained (2 seconds longer) response compared to the *pdfGAL4* driven response (Figure 5F). AgCRY1 generates sustained depolarized light responses when expressed by the *pdfGAL4* driver line and a sustained and more rapid response when expressed in all CRY neurons (light purple and purple traces, respectively, Figure 5G) as compared to *cry-null* evoked responses (grey trace, Figure 5E). AgCRY1 mediates cell-autonomous light responses in the LNvs, while AeCRY1 does not. The sustained AgCRY1 evoked response is another feature of its greater light sensitivity than AeCRY1 (Figure 5F, G). All CRYs tested exhibit higher magnitude and more sustained light evoked potentials when expressed broadly using the *crypGAL4–24* driver relative to LNv restricted expression by the *pdfGAL4* driver. Representative 1-minute l-LNv patch clamp voltage traces are shown in Figure S5 and S6.

Insects exhibit species-specific light attraction/avoidance behavioral responses over the spectral range between ultraviolet to red[7,14,20,21,32,33,41–45]. Spectral absorption analysis of *in vitro* purified DmCRY in the FAD oxidized and FAD•- anionic semiquinone states exhibit peaks around 365 and 450 nm that correspond to UV and blue [23,46–48]. However, we recently demonstrated in *ex vivo* patch clamp recordings that DmCRY mediates electrophysiological responses to red light (635 nm) that are absent in recordings made from the brains of *cry-null* flies and wild type flies treated with the redox sensitive flavin specific inhibitor diphenyleneiodonium (DPI)[20]. These results suggest that *in situ* DmCRY in its native neuronal environment expresses the further reduced FADH• neutral semiquinone state that exhibits red light absorption and biological activity[27]. Diurnal *Ae. aegypti* female mosquitoes show no differences between UV, blue or red-light attraction behavior during the day, while nocturnal *An. coluzzii* female mosquitoes strongly avoid UV and blue light, but are significantly attracted to red light during the day[33]. *Ae. aegypti* mosquitoes also exhibit strong attraction and image discrimination towards red-colored objects as part of their image-forming vision for prey detection[7]. To test the hypothesis that nocturnal AgCRY1 is red light responsive, but diurnal AeCRY1 is not, we expressed AgCRY1, AeCRY1 and DmCRY using the *crypGAL4–24* driver, along with *cry-null* controls and measured the electrophysiological changes of l-LNvs in response to 200 μW/cm^2 red light stimulation for all genotypes. Red light evokes significant increases in firing rate in flies expressing AgCRY1 and flies expressing DmCRY relative to *cry-null* (Figure 6A). In contrast, AeCRY1 lacks a red light FF electrophysiological response and is significantly lower relative to

AgCRY1 (Figure 6A, C). The red light evoked potential response of DmCRY is robust, with a sharp spike in membrane potential at the onset of light that lasts 10 seconds that returns to baseline rapidly (Figure 6B). Negative control *cry-null* flies completely lack a red light response (Figure 6A, B, D). Comparing the FF ratio during stimulus and several 10-second bins post-stimulus along with red light evoked potentials, we observed a rapid decay (<10 seconds) back to baseline for red light with DmCRY and AgCRY1 flies, and a lack of sustained response for AeCRY1 and *cry-null* flies (Figure 6B–E). These results confirm and extend findings showing that insect CRY1s *in situ* are capable of biological responses to red light. Representative 1-minute l-LNv patch clamp voltage traces are shown in Figure S7. Blue and UV light pulses evoking long duration l-LNvs depolarization mediated by DmCRY are associated with behavioral photoavoidance of UV light in flies and nocturnal mosquitoes, while the much shorter duration red light evoked depolarization mediated by AgCRY1 may code for behavioral phototaxis in *Anopheline* mosquitoes[33].

Mosquito CRY1s confer species-specific and intensity-dependent behavioral attraction/avoidance to UV light

Nocturnal mosquitoes exhibit strong daytime behavioral avoidance of UV light, while diurnal mosquitoes exhibit strong daytime attraction to UV light[33]. To explore CRY1's potential role for conferring nocturnal versus diurnal mosquito species-specific light choice behaviors, we performed a UV light choice behavioral assay with flies expressing DmCRY, AgCRY1, AeCRY1 under the *crypGAL4–24* promoter at three different light intensities. At very low intensity 365 nm UV light (1 μW/cm^2) during the first 30 minutes of light choice preference, all groups show no differences and are attracted to the very low intensity UV light exposed side (Figure 7A). At moderately low-intensity UV light (10 μW/cm^2), the genotypes begin to diverge: DmCRY and diurnal AeCRY1 expressing flies prefer the light exposed side and do not differ between each other (Figure 7B), but the nocturnal AgCRY1 exhibit significant light avoidance to the 10 μW/cm^2 UV light exposed environment, with approximately 50–60% of flies being in the shaded environment during daytime hours (Figure 7B). At high-intensity UV light (400 μW/cm^2), AgCRY1 flies increase avoidance to the UV exposed environment and DmCRY flies shift to exhibit light avoidance behaviors (Figure 7C). However, the AeCRY1 flies remain significantly attracted to the high intensity UV light environment (Figure 7C). These results show a sensitivity threshold for UV light avoidance response for AgCRY1 flies at 10 μW/cm^2, compared to the 400 μW/cm^2 threshold for the UV light avoidance response for DmCRY flies as reported previously[11,21,32]. These results are not due to differences in the number of LNvs in the brain that express CRY or TIM (Figure S3). We integrated all mean activity starting at lights on through 30 minutes for paired t-test analysis represented as bar graphs in D, E, F in Figure 7, showing significant differences between AgCRY1 and AeCRY1 expressing flies at all light intensities tested. The UV light intensity dependent divergence between AeCRY1 and AgCRY1 expressing flies for the light attraction/avoidance assay is highly consistent with the behavioral results of the same assay testing diurnal and nocturnal mosquitoes and supports our hypothesis that CRY photoreceptors mediate species-specific physiological and behavioral light responses.

Discussion

These findings highlight CRY as a strong species-specific behavioral regulator of behavioral light responses shown by a wide range of physiological and behavioral assays. *Drosophila* CRY- and diurnal/nocturnal mosquito CRY1- mediated behavioral light responses and electrophysiological responses provide strong support for the idea that CRY mediates light responses by species-specific mechanisms that have evolved to optimize survival by time-of-day specific feeding, mating, and predatory avoidance behaviors. *Ae. aegypti* and *An. gambiae* mosquitoes are active at 12 hr opposing times of the day[33]. *Ae. aegypti* are aggressive daytime biters, while nocturnal *An. Gambiae* prefer to feed on defenseless sleeping prey. *Ae. aegypti* mosquitoes are attracted to a wide range of light spectra during the daytime, while *An. gambiae* mosquitoes specifically avoid short-wavelength light during the day, but exhibit daytime attraction to red light. We conclude that CRY1 from nocturnal *An. gambiae* exhibits greater light sensitivity than CRY1 from diurnal *Ae. aegypti*, and that these functional differences contribute to their distinct species-specific light responses.

SUPPLEMENTAL INFORMATION

RESOURCE AVAILABILITY

Lead Contact—Further information and requests for resources and reagents should be directed to and will be fulfilled by the Lead Contact, Prof. Todd C. Holmes (tholmes@uci.edu)

Materials Availability—Upon publication, the UAS-DmCRY, UAS-AeCRY1 and UAS-AgCRY1 transgenic *Drosophila* will be deposited at the Bloomington Stock Center, further information and requests for resources should be directed to the Lead Contact.

Data and Code Availability

- Original data is available upon request to the corresponding author.
- Code used for statistical analysis will be deposited to the UCI Center for Neural Circuit Mapping website at https://cncm.som.uci.edu/
- Any additional information required to reanalyze the data reported in this paper is available from the lead contact upon request.

Experimental Model and Subject Details

***Drosophila* maintenance:** Fruit flies *D. melanogaster* were raised on standard media (yeast, cornmeal, agar) at 25±1 °C and 40–60% relative humidity in 12:12h light/dark cycles. All flies used in experiments were backcrossed for six generations to the w1118 genetic background. Detailed information on fly crosses is indicated in the relevant Method Details. All behavioral experiments used 3–4-day old flies. For strain details please see Key Resources Table.

METHOD DETAILS

Experimental animals—We created synthetic DNA constructs (Genscript) using a pJFRC7 vector containing the full *Drosophila* cryptochrome sequence, in frame with eGFP (Addgene). Generation of constructs containing cryptochrome 1 from *An. gambiae* (Ag) and *Ae. aegypti* (Ae) in frame with eGFP were also performed this way. DmCRY-eGFP, AgCRY1-eGFP, and AeCRY1-eGFP constructs using the pJFRC7 vector allow for a controlled insertion into the same genomic location via a specific PhiC31 genomic site. The synthetic DNA constructs containing each cryptochrome-eGFP variant were injected into fly embryos, reared, then screened for eye color as evidence of successful transgenesis. Resultant transgenic flies were isogenized by backcrossing with w1118 flies for a minimum of 6 generations. The following primers were designed to genotype-verify successful transgene insertion: AeCRY1 Forward: CGA GAA AGT GCA GGC CAA CAA TC, AeCRY1 Reverse: GT TCT TCA ACT CCG GCA GAT ATC, AgCRY1 Forward: CAG CCA GTT CAA GTA TCC GG, and AgCRY1 Reverse: CGG TTC GTG CAC AAA CTG TG. For quality control, DNA constructs were sequenced before embryonic insertion and gDNA from transgenic flies after embryonic insertion (GeneWiz). All vectors were injected into *Drosophila* embryos (BestGene) to generate the UAS-eGFP-DmCRY, UAS-eGFP-AgCRY1, and UAS-eGFP-AeCRY1 transgenic flies. Each transgenic fly line was crossed into a *cry-null* background (obtained from Jeff Hall, Brandeis University) and again with a *pdfGAL4* or *crypGAL4–24* flies to generate the final transgenic mutant lines expressing DmCRY or mosquito CRY1 under a pdf- or cry-driver in a *cry-null* background.

Immunocytochemistry—Flies were entrained at 12:12 hr LD conditions for 3–5 days before males were separated and CO2 anesthetized for dissection. Dissections began approximately 1 hour before each respective ZT timepoint (ZT5, 11, 17, 23). To minimize introducing variance by circadian timing or experimental differences, all flies were entrained and dissected at the same time and days. Dissections were carried out at the same time for all genotypes tested and were repeated over 3 total experimental repeats. Brains were dissected in chilled 1X PBS, fixed in 4% paraformaldehyde (PFA) for 30min, washed 3X 10min in PBS-Triton-X 1%, incubated in blocking buffer (10% Horse Serum-PBS-Triton-X 0.5%) at room temperature before incubation with rabbit α-TIM, polyclonal (1:1,000) antibodies overnight in 4°C. Brains were washed 3X 10min in PBS-Triton-X 0.5% then incubated in goat α-rabbit-Alexa- 594 (1:1,000) secondary antibodies in blocking buffer overnight in 4°C. Brains were washed 5X 15min in PBS-Triton-X 0.5% before mounting in Vectashield mounting media (Vector Laboratories). Microscopy was performed using a Leica SP8 confocal microscope.

Locomotor Activity Behavior Assay—For our constant light behavior experiments, we used an adapted fly locomotor activity protocol[55,56]. Adult male flies were selected at 2–4 days post-eclosion then loaded in individual locomotor activity tubes. Locomotor activity of individual flies was measured using the TriKinetics Locomotor Activity Monitoring System via infrared beam-crossing recording total crosses in 30 min bins. Flies were initially entrained in 12:12 hr light:dark (LD) condition for 7 days, then they were exposed to 7 days of constant light (LL) conditions. Actograms were generated using Clocklab software. Average activity eduction graphs and its statistics were measured using FaasX software,

then graphed using Microsoft Excel. Within FaasX, the CycleP analysis toolkit was used to calculate tau (τ), rhythm power, and period width via periodogram analysis with the following scoring criteria for flies in LL: minimum power ≥ 20, minimum width (h) ≥ 2, Chi-square significance ≥ 0.05. Data are reported as approximations of means.

Light-Evoked Neuronal Electrophysiology—Electrophysiology whole-cell current-clamp recordings were carried out from previously established and adapted protocols[20]. Adult male (3–5 days post-eclosion) fly brains were dissected in external recording solution. l-LNvs were subjected to whole-cell current-clamp with external solution: 122mM NaCl, 3mM KCl, 1.8mM CaCl2, 0.8mM MgCl2, 5mM glucose, 10mM HEPES, 7.2 pH, and 250–255mOsm; internal solution: 102mM Kgluconate, 17mM NaCl, 0.085mM CaCl2, 1.7mM MgCl2 (hexahydrate), 8.5mM HEPES, 0.94mM EGTA, 7.2pH, and 232–235mOsm. Custom-ordered multichannel LED source (Prizmatix/Stanford Photonics, Palo Alto, CA) fitted to the Olympus BX51 WI microscope was used for all optics using electrophysiology recordings. LED peak wavelengths are as follows: UV (365 nm) blue (450 nm), and red (635 nm), and all exposures were set to intensity of 200 μW/cm2. Lower light intensities (20, 2, 0.2 μW/cm2) were adjusted using GamColor CineFilter 1516 .6 neutral density filters placed against the light source. Light intensities were determined by a Newport 842-PE Power/Energy meter. Each LED was triggered on and off for each sweep with TTL pulses programmed by pClamp (Molecular Dynamics) data acquisition software. Each color pulse was 5 seconds long. Each light pulse was preceded by minimum 50 second pre-pulse dark baseline, and there was 95 second inter-pulse intervals between each light exposure from there on, with 5–10 times of each color exposed per cell. All sweeps containing each light exposure recordings were averaged, and baseline was adjusted to pre-pulse signal. Furthermore, Gaussian and Butterworth filters were applied to the averaged signals using the ClampFit 10 software (Molecular Dynamics). The light evoked potential protocol collects individual baseline pre-stimulus recordings of membrane potential in current clamp mode and during the 5 second LED light stimulus, followed by 45–90 seconds of post light stimulus recording of membrane potential. The light pulse is repeated multiple times and all individual recordings for a given genotype and light stimulus are time locked to the light pulse duration, then averaged to capture averaged light evoked changes in membrane potential measured in millivolts [20,22], thus providing a kinetically robust light evoked potential.

UV Light Attraction/Avoidance Behavior Assay—Standard LD light choice assays were conducted from previously established and adapted protocols[21]. The locomotor activity of individual flies was measured using the TriKinetics Locomotor Activity Monitoring System via infrared beam-crossing, recording total crosses in 1-min bins. Percentage activity and statistics were measured using Microsoft Excel. Philips TL-D Blacklight UV source with a narrow peak wavelength of 365 nm and intensity of 400 μW/cm2 was used for high intensity, and 10 μW/cm2 was used for low intensity by using neutral-density filters.

Confocal microscopy and Image processing—Brains were imaged with Leica SP8 confocal microscope. Images were quantified with ImageJ by selecting all regions of CRY-expressing/GFP-positive neurons for *crypGAL4–24* driven transgenic flies, or PDF-

expressing/GFP-positive neurons for *pdfGAL4* driven transgenic flies. Maximum intensity projections were created using the Z stack tool between the image slices corresponding to the brain. Fluorescence from each brain were calculated by normalizing the mean intensities of the neurons against the background region of the brain. Only TIM fluorescence was quantified for the *cry-null* negative control flies, because there was no clear GFP expression to be able to identify those neurons. All images are adjusted for clarity with +40% Brightness and −20% Contrast from the original images.

Protein Sequence Alignment—Protein BLAST comparison in Figure S1 was generated by using FASTA sequences obtained from NCBI Protein Database for DmCRY (Accession: NP_732407), AgCRY1 (Accession: ABB29886), and AeCRY1 (Accession: Q17DK5). Sequences were aligned using a third party T-coffee multiple alignment tool (https://tcoffee.crg.eu/apps/tcoffee/do:regular) and color formatted using a BoxShade toolkit (https://www.ch.embnet.org/software/BOX_form.html).

QUANTIFICATION AND STATISTICAL ANALYSIS

Data are presented as mean ± SEM. Values of n refer to the total number of tested flies. In all cases, the n values were obtained from at least three separate experiments. Firing frequency data are reported as a ratio of spike events occurring during the 5 seconds of lights on/average spike events in the preceding 50 seconds binned in 10 second increments. Light-evoked increases of FF are significantly greater than the baseline FF ratio of 1. This was done to normalize across individual preparations. Statistical tests were performed using Minitab, Matlab, and Microsoft Excel software. Data were established as normally distributed through Anderson-Darling normality tests. For pairwise comparisons: F-tests were used to determine equal or unequal variance for normally distributed data, and one-tailed T-tests were used to determine significance between groups. Otherwise, for nonparametric data Mann-Whitney U-tests were run to determine significance between groups. For multi-group comparison: Barlett's test was used on normally distributed data and the Brown-Forsythe test was used on nonnormally distributed data to determine equivalence of variance. Significance within normally distributed data having equal variance was determined with one-way ANOVA and post-hoc Tukey test analysis, whereas Games-Howell was run for post-hoc analysis on data with unequal variance. Nonparametric tests to determine significance for data with equal and unequal variance was determined with Kruskal-Wallis one-way analysis of variance and post-hoc analysis using Dunn's test. Firing frequency analysis on electrophysiological recordings were performed using a custom Matlab script. To ensure Type I errors, i.e., false positives, are not inflated by the multiple comparisons, we computed the adjusted p-values based on an approach that controls the false discovery rate (FDR[57]). A commonly used threshold 0.1 indicates that among the ones reported significant, the expected proportion of false positives is no greater than 10%. Membrane potential statistical analysis was simplified by binning each timepoint into 1 second average signal responses, then performing the appropriate statistical tests/post-hoc analyses based on normal distribution and equivalence of variance for each individual timepoint. These calculations were streamlined using custom Matlab scripts and excel spreadsheet.

Supplementary Material

Refer to Web version on PubMed Central for supplementary material.

Acknowledgements

We thank Francesco Tombola, Kevin Beier, and Brian Zoltowski for helpful discussions; Lisa Baik for research support; Jerry Houl for help generating transgenic lines; Mai Doan for analytical and statistical support; Parrish Powell for lab managerial support; Janita Parpana, Duke Park, Lillian Li, and Claire Chen for administrative support. T.C.H. is supported by R35 GM127102. D.D.A. acknowledges partial support by an individual NIH NRSA fellowship F31 GM140592.

References

1. Whitfield J Portrait of a serial killer. Nature (2002) 10.1038/news021001-6
2. Bidlingmayer WL (1994) How Mosquitoes See Traps: Role of Visual Responses. J. Am. Mosq. Control Assoc. 10, 272–279. [PubMed: 8965079]
3. Ditzen M, Pellegrino M, and Vosshall LB (2008) Insect Odorant Receptors Are Molecular Targets of the Insect Repellent DEET. Science 319, 1838–1842. [PubMed: 18339904]
4. Lazzari CR (2009) Chapter 1 Orientation Towards Hosts in Haematophagous Insects. In Advances in Insect Physiology; Elsevier; 37, 1–58.
5. McMeniman CJ, Corfas RA, Matthews BJ Ritchie SA, and Vosshall LB (2014) Multimodal Integration of Carbon Dioxide and Other Sensory Cues Drives Mosquito Attraction to Humans. Cell 156, 1060–1071. [PubMed: 24581501]
6. Raji JI and DeGennaro M (2017) Genetic Analysis of Mosquito Detection of Humans. Curr. Opin. Insect Sci 20, 34–38. [PubMed: 28428935]
7. Alonso San Alberto D, Rusch C, Zhan Y, Straw AD, Montell C, and Riffell JA (2022) The Olfactory Gating of Visual Preferences to Human Skin and Visible Spectra in Mosquitoes. Nat. Commun. 13, 555–569. [PubMed: 35121739]
8. Blondell J (1997) Epidemiology of Pesticide Poisonings in the United States, with Special Reference to Occupational Cases. Occup. Med. Phila. 12, 209–220.
9. Garey J and Wolff MS (1998) Estrogenic and Antiprogestagenic Activities of Pyrethroid Insecticides. Biochem. Biophys. Res. Commun. 251, 855–859. [PubMed: 9790999]
10. Hemingway J and Ranson H (2000) Insecticide Resistance in Insect Vectors of Human Disease. Annu. Rev. Entomol. 45, 371–391. [PubMed: 10761582]
11. Baik LS, Recinos Y, Chevez JA, Au DD and Holmes TC (2019) Multiple Phototransduction Inputs Integrate to Mediate UV Light–Evoked Avoidance/Attraction Behavior in Drosophila. J. Biol. Rhythms 34, 391–400. [PubMed: 31140349]
12. Fogle KJ, Baik LS, Houl JH, Tran TT, Roberts L, Dahm NA, Cao Y, Zhou M and Holmes TC (2015) CRYPTOCHROME-Mediated Phototransduction by Modulation of the Potassium Ion Channel β-Subunit Redox Sensor. Proc. Natl. Acad. Sci. 112, 2245–2250. [PubMed: 25646452]
13. Garbe DS, Bollinger WL, Vigderman A, Masek P, Gertowski J, Sehgal A and Keene AC (2015) Context-Specific Comparison of Sleep Acquisition Systems in Drosophila. Biol. Open 4, 1558–1568. [PubMed: 26519516]
14. Keene AC, Mazzoni EO, Zhen J, Younger MA, Yamaguchi S, Blau J, Desplan C and Sprecher SG (2011) Distinct Visual Pathways Mediate Drosophila Larval Light Avoidance and Circadian Clock Entrainment. J. Neurosci. 31, 6527–6534. [PubMed: 21525293]
15. Klarsfeld A, Picot M, Vias C, Chelot E and Rouyer F (2011) Identifying Specific Light Inputs for Each Subgroup of Brain Clock Neurons in Drosophila Larvae. J. Neurosci. 31, 17406–17415. [PubMed: 22131402]
16. Miller GV, Hansen KN and Stark WS (1981) Phototaxis in Drosophila: R1–6 Input and Interaction among Ocellar and Compound Eye Receptors. J. Insect Physiol. 27, 813–819.

17. Sheeba V, Fogle KJ, Kaneko M, Rashid S, Chou Y-T, Sharma VK and Holmes TC (2008) Large Ventral Lateral Neurons Modulate Arousal and Sleep in Drosophila. Curr. Biol. 18, 1537–1545. [PubMed: 18771923]
18. Gao S, Takemura S, Ting C-Y, Huang S, Lu Z, Luan H, Rister J, Thum AS, Yang M, Hong S-T et al. (2008) The Neural Substrate of Spectral Preference in Drosophila. Neuron 60, 328–342. [PubMed: 18957224]
19. Yamaguchi S, Desplan C and Heisenberg M (2010) Contribution of Photoreceptor Subtypes to Spectral Wavelength Preference in Drosophila. Proc. Natl. Acad. Sci. 107, 5634–5639. [PubMed: 20212139]
20. Baik LS, Au DD, Nave C, Foden AJ, Enrriquez-Villalva WK and Holmes TC (2019) Distinct Mechanisms of Drosophila CRYPTOCHROME-Mediated Light-Evoked Membrane Depolarization and in Vivo Clock Resetting. Proc. Natl. Acad. Sci. 116, 23339–23344. [PubMed: 31659046]
21. Baik LS, Fogle KJ, Roberts L, Galschiodt AM, Chevez JA, Recinos Y, Nguy V and Holmes TC (2017) CRYPTOCHROME Mediates Behavioral Executive Choice in Response to UV Light. Proc. Natl. Acad. Sci. 114, 776–781. [PubMed: 28062690]
22. Fogle KJ, Parson KG, Dahm NA and Holmes TC (2011) CRYPTOCHROME Is a Blue-Light Sensor That Regulates Neuronal Firing Rate. Science 331, 1409–1413. [PubMed: 21385718]
23. Hoang N, Schleicher E, Kacprzak S, Bouly J-P, Picot M, Wu W, Berndt A, Wolf E, Bittl R and Ahmad M (2008) Human and Drosophila Cryptochromes Are Light Activated by Flavin Photoreduction in Living Cells. PLoS Biol. 6, e160. [PubMed: 18597555]
24. Levy C, Zoltowski BD, Jones AR, Vaidya AT, Top D, Widom J, Young MW, Scrutton NS, Crane BR and Leys D (2013) Updated Structure of Drosophila Cryptochrome. Nature 495, E3–E4. [PubMed: 23518567]
25. Lin C, Top D, Manahan CC, Young MW and Crane BR (2018) Circadian Clock Activity of Cryptochrome Relies on Tryptophan-Mediated Photoreduction. Proc. Natl. Acad. Sci. 115, 3822–3827. [PubMed: 29581265]
26. Zoltowski BD, Vaidya AT, Top D, Widom J, Young MW and Crane BR (2011) Structure of Full-Length Drosophila Cryptochrome. Nature 480, 396–399. [PubMed: 22080955]
27. Öztürk N, Song S-H, Selby CP and Sancar A (2008) Animal Type 1 Cryptochromes. J. Biol. Chem. 283, 3256–3263. [PubMed: 18056988]
28. Benito J, Houl JH, Roman GW and Hardin PE (2008) The Blue-Light Photoreceptor CRYPTOCHROME Is Expressed in a Subset of Circadian Oscillator Neurons in the Drosophila CNS. J. Biol. Rhythms 23, 296–307. [PubMed: 18663237]
29. Emery P, So WV, Kaneko M, Hall JC and Rosbash M (1998) CRY, a Drosophila Clock and Light-Regulated Cryptochrome, Is a Major Contributor to Circadian Rhythm Resetting and Photosensitivity. Cell 95, 669–679. [PubMed: 9845369]
30. Sheeba V, Gu H, Sharma VK, O'Dowd DK and Holmes TC (2008) Circadian- and Light-Dependent Regulation of Resting Membrane Potential and Spontaneous Action Potential Firing of Drosophila Circadian Pacemaker Neurons. J. Neurophysiol. 99, 976–988. [PubMed: 18077664]
31. Yoshii T, Todo T, Wülbeck C, Stanewsky R and Helfrich-Förster C (2008) Cryptochrome Is Present in the Compound Eyes and a Subset OfDrosophila's Clock Neurons. J. Comp. Neurol. 508, 952–966. [PubMed: 18399544]
32. Baik LS; Recinos Y; Chevez JA and Holmes TC (2018) Circadian Modulation of Light-Evoked Avoidance/Attraction Behavior in Drosophila. PLOS ONE 13, e0201927. [PubMed: 30106957]
33. Baik LS, Nave C, Au DD, Guda T, Chevez JA, Ray A and Holmes TC (2020) Circadian Regulation of Light-Evoked Attraction and Avoidance Behaviors in Daytime- versus Nighttime-Biting Mosquitoes. Curr. Biol. 30, 3252–3259. [PubMed: 32619483]
34. Koh K, Zheng X and Sehgal A (2006) JETLAG Resets the Drosophila Circadian Clock by Promoting Light-Induced Degradation of TIMELESS. Science 312, 1809–1812. [PubMed: 16794082]
35. Petersen G, Hall JCand Rosbash M (1988) The Period Gene of Drosophila Carries Species-Specific Behavioral Instructions. EMBO J. 7, 3939–3947. [PubMed: 3208755]

36. Wheeler DA, Kyriacou CP, Greenacre ML, Yu Q, Rutila JE, Rosbash M and Hall JC (1991) Molecular Transfer of a Species-Specific Behavior from Drosophila Simulans to Drosophila Melanogaster. Science 251, 1082–1085. [PubMed: 1900131]
37. Tauber E, Roe H, Costa R, Hennessy JM and Kyriacou CP (2003) Temporal Mating Isolation Driven by a Behavioral Gene in Drosophila. Curr. Biol. 13, 140–145. [PubMed: 12546788]
38. Dobritsa AA, van der Goes van Naters W, Warr CG, Steinbrecht RA and Carlson JR (2003) Integrating the Molecular and Cellular Basis of Odor Coding in the Drosophila Antenna. Neuron 37, 827–841. [PubMed: 12628173]
39. Hallem EA, Ho MG and Carlson JR (2004) The Molecular Basis of Odor Coding in the Drosophila Antenna. Cell 117, 965–979. [PubMed: 15210116]
40. Helfrich-Förster C (1998) Robust Circadian Rhythmicity of Drosophila Melanogaster Requires the Presence of Lateral Neurons: A Brain-Behavioral Study of Disconnected Mutants. J. Comp. Physiol. [A] 182, 435–453.
41. Zhao J, Kilman VL, Keegan KP, Peng Y, Emery P, Rosbash M and Allada R (2003) Drosophila Clock Can Generate Ectopic Circadian Clocks. Cell 113, 755–766. [PubMed: 12809606]
42. Dolezelova E, Dolezel D and Hall JC (2007) Rhythm Defects Caused by Newly Engineered Null Mutations in Drosophila's Cryptochrome Gene. Genetics 177, 329–345. [PubMed: 17720919]
43. Rakshit K and Giebultowicz JM (2013) Cryptochrome Restores Dampened Circadian Rhythms and Promotes Healthspan in Aging Drosophila. Aging Cell 12, 752–762. [PubMed: 23692507]
44. Zhu H, Yuan Q, Froy O, Casselman A and Reppert SM (2005) The Two CRYs of the Butterfly. Curr. Biol. 15, R953–R954. [PubMed: 16332522]
45. Yuan Q, Metterville D, Briscoe AD and Reppert SM (2007) Insect Cryptochromes: Gene Duplication and Loss Define Diverse Ways to Construct Insect Circadian Clocks. Mol. Biol. Evol. 24, 948–955. [PubMed: 17244599]
46. Chandler JA; Hill MN and Highton RB (1976) The Use of Light Traps for Long-Term Surveillance of Mosquitoes of Epidemiological Importance on the Kano Plain, Kenya. East Afr. Med. J. 53, 596–600. [PubMed: 13987]
47. Doukas D and Payne CC (2007) The Use of Ultraviolet-Blocking Films in Insect Pest Management in the UK; Effects on Naturally Occurring Arthropod Pest and Natural Enemy Populations in a Protected Cucumber Crop. Ann. Appl. Biol. 151, 221–231.
48. Grant GG; Carmichael AG; Smith CN and Brown AWA (1970) Autochemosterilization of the Southern House Mosquito by Means of a Modified Light Trap. J. Econ. Entomol. 63, 648–650. [PubMed: 5462415]
49. Jawara M, Awolola TS, Pinder M, Jeffries D, Smallegange RC, Takken W and Conway DJ (2011) Field Testing of Different Chemical Combinations as Odour Baits for Trapping Wild Mosquitoes in The Gambia. PLoS ONE 6, e19676. [PubMed: 21637337]
50. Pickens LG (1989) Relative Attractiveness of Paired BL and BLB Fluorescent Bulbs for House and Stable Flies (Diptera: Muscidae). J. Econ. Entomol. 82, 535–538. [PubMed: 2708631]
51. Berndt A, Kottke T, Breitkreuz H, Dvorsky R, Hennig S, Alexander M and Wolf E (2007) A Novel Photoreaction Mechanism for the Circadian Blue Light Photoreceptor Drosophila Cryptochrome. J. Biol. Chem. 282, 13011–13021. [PubMed: 17298948]
52. Bouly J-P, Schleicher E, Dionisio-Sese M, Vandenbussche F, Van Der Straeten D, Bakrim N, Meier S, Batschauer A, Galland P, Bittl R et al. (2007) Cryptochrome Blue Light Photoreceptors Are Activated through Interconversion of Flavin Redox States. J. Biol. Chem. 282, 9383–9391. [PubMed: 17237227]
53. Liu B, Liu H, Zhong D and Lin C (2010) Searching for a Photocycle of the Cryptochrome Photoreceptors. Curr. Opin. Plant Biol. 13, 578–586. [PubMed: 20943427]
54. Ni JD, Baik LS, Holmes TC and Montell CA (2017) Rhodopsin in the Brain Functions in Circadian Photoentrainment in Drosophila. Nature 545, 340–344. [PubMed: 28489826]
55. Chiu JC, Low KH, Pike DH, Yildirim E and Edery I (2010) Assaying Locomotor Activity to Study Circadian Rhythms and Sleep Parameters in Drosophila. J. Vis. Exp. 43, 2157.
56. Nitabach MN, Blau J and Holmes TC (2002) Electrical silencing of central pacemaker neurons stops the central molecular clock. Cell 109,485–495. [PubMed: 12086605]

57. Benjamini Y and Hochberg Y (1995) Controlling the False Discovery Rate: A Practical and Powerful Approach to Multiple Testing. J. R. Stat. Soc. Ser. B Methodol. 57, 289–300.

Highlights

- Nocturnal *Anopheles gambiae* and diurnal *Aedes aegypti* express light active CRY1s
- *An.gambiae* CRY1 shows greater behavioral light responses than *Ae.aegypti* CRY1
- Greater *An.gambiae* CRY1 electrophysiological light responses than *Ae.aegypti* CRY1

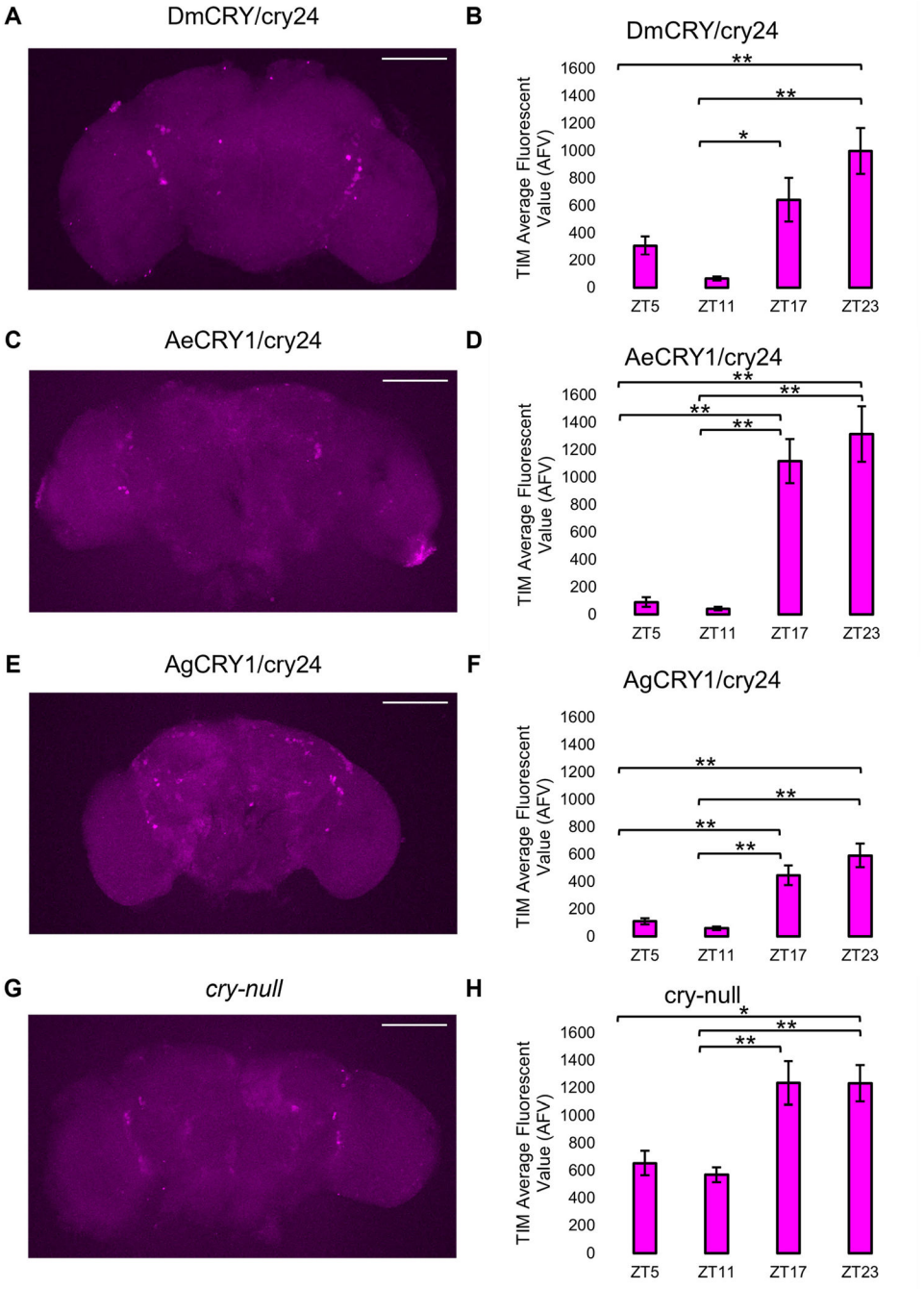

Figure 1. AeCRY1 and AgCRY1 expression does not disrupt the peak time of the circadian clock in transgenic flies

Immunocytochemistry average fluorescent value of TIM expression over 12:12 hr LD at ZT 5, 11, 17, and 23 timepoints in LNvs expressing (A, B) DmCRY with representative image, (C, D) AeCRY1 with representative image, (E, F) AgCRY1 with representative image over *cry-null* background, and (G, H) negative control *cry-null*. All representative images are at ZT 23, have a 100-micron scale bar for reference, and have been modified for clarity with 40% brightness and −20% contrast. Data are represented as mean ± SEM. * $p \leq 0.05$, ** $p \leq 0.005$, ***$p \leq 0.001$. See also Figures S2 and S3.

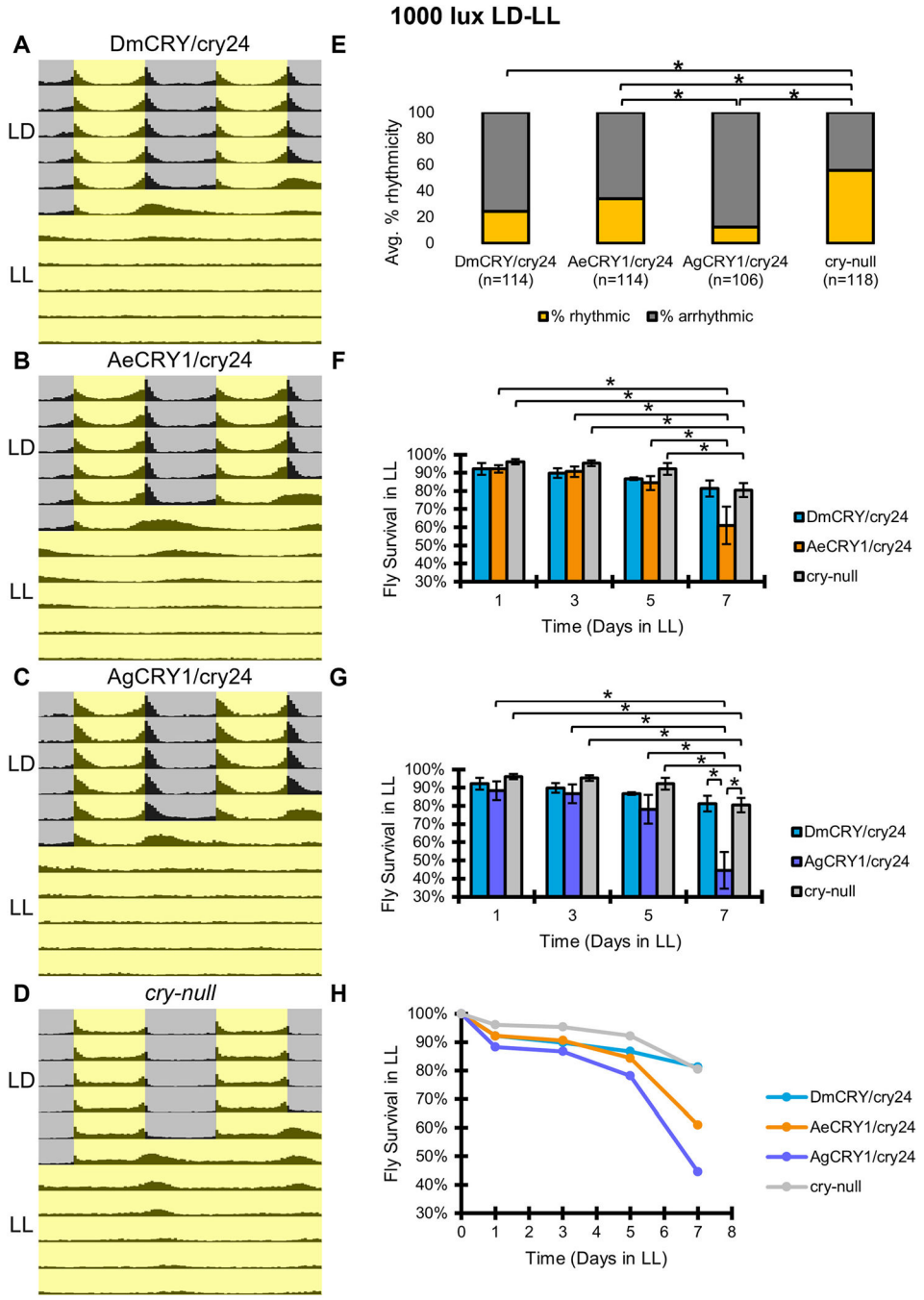

Figure 2. AgCRY1 and control DmCRY expressing flies are arrhythmic in high intensity constant light (1000 lux LL), AeCRY1 expressing flies are partial arrhythmic and *cry-null* flies remain rhythmic in LL

(A-D) Actograms plots containing 5 days of 12:12 hr LD entrainment followed by 5 days of high intensity constant light (1000 lux LL) conditions for flies expressing: (A) DmCRY (n=114; τ_{avg}≈25.2, $power_{avg}$≈51.0, $width_{avg}$≈3.4), (B) AeCRY1 (n=114; τ_{avg}≈25.4, $power_{avg}$≈47.6, $width_{avg}$≈4.2), (C) AgCRY1 (n=106; τ_{avg}≈25.1, $power_{avg}$≈34.4, $width_{avg}$≈2.4), (D) *cry-null* (n=118; τ_{avg}≈25.1, $power_{avg}$≈67.4, $width_{avg}$≈3.6). (E) Quantification of fly rhythmicity (orange) to arrhythmicity (grey) in LL. (F-H) Fly survival

plots over an extended 7-day period of high intensity LL exposure: (F) Bar charts of the average survival percentage at days 1, 3, 5, and 7 in LL of DmCRY (blue) vs AeCRY1 (orange) vs *cry-null* (grey) groups. (G) Bar charts of the average survival percentage at days 1, 3, 5, and 7 in LL of DmCRY vs AgCRY1 (purple) vs *cry-null* groups. (H) Line plot summary of LL survivability for both AeCRY1 and AgCRY1 groups compared with DmCRY and *cry-null*. Data are represented as mean ± SEM. *$p \leq 0.05$, **$p \leq 0.005$, ***$p \leq 0.001$.

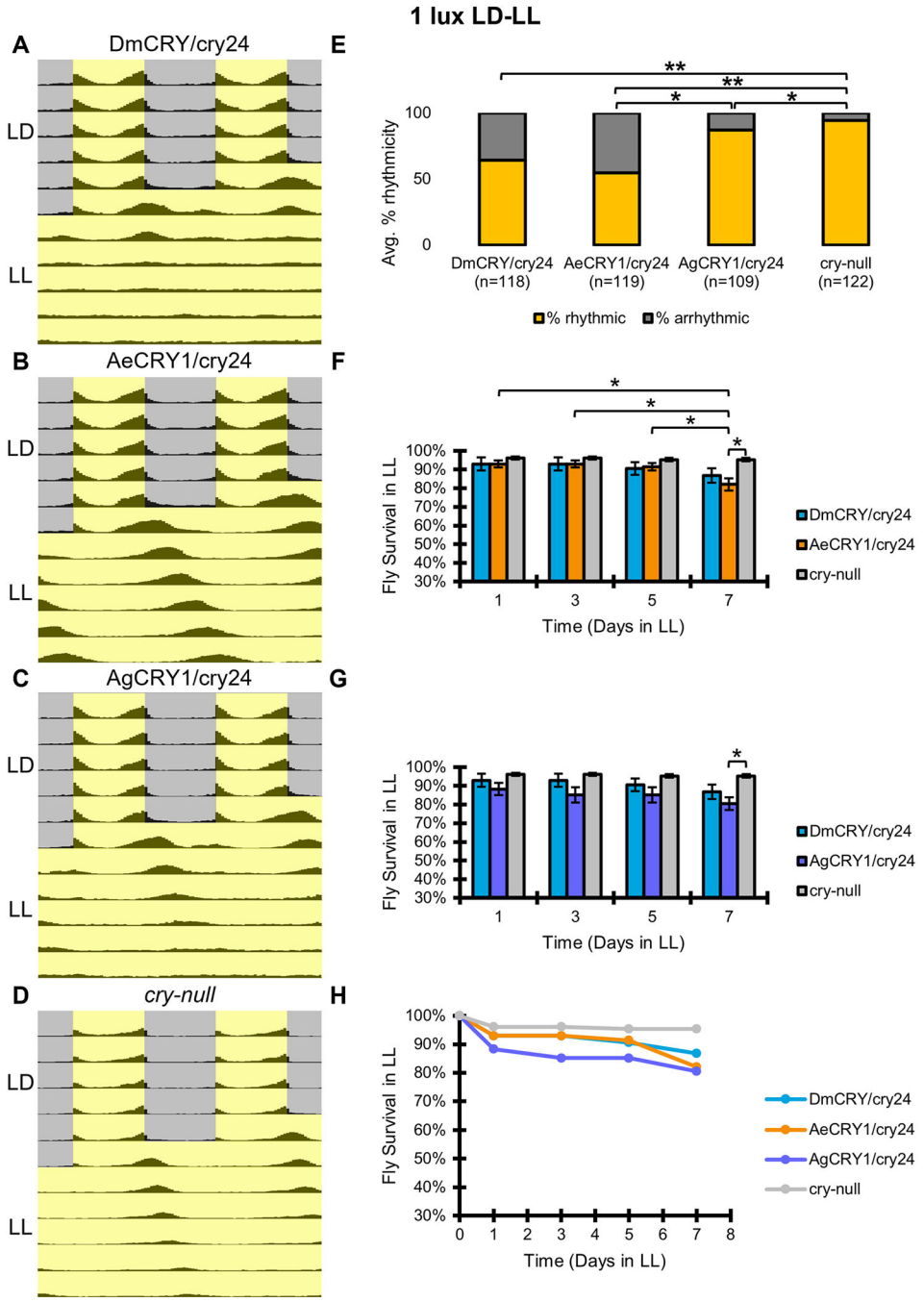

Figure 3. AeCRY1 and control DmCRY expressing flies are partial arrhythmic in low intensity constant light (1 lux LL), AgCRY1 and *cry-null* flies remain highly rhythmic in LL

(A-D) Actograms plots containing 5 days of 12:12 hr LD entrainment followed by 5 days of low intensity constant light (1 lux LL) conditions for flies expressing: (A) DmCRY (n=118; τ_{avg}≈24.9, $power_{avg}$≈62.5, $width_{avg}$≈3.2), (B) AeCRY1 (n=119; τ_{avg}≈26.0, $power_{avg}$≈118.0, $width_{avg}$≈5.6), (C) AgCRY1 (n=109; τ_{avg}≈26.0, $power_{avg}$≈68.0, $width_{avg}$≈4.3), (D) *cry-null* (n=122; τ_{avg}≈25.2, $power_{avg}$≈109.8, $width_{avg}$≈5.2). (E) Quantification of fly rhythmicity (orange) to arrhythmicity (grey) in LL. (F-H) Fly survival plots over an extended 7-day period of low intensity LL exposure: (F) Bar charts of the

average survival percentage at days 1, 3, 5, and 7 in LL of DmCRY (blue) vs AeCRY1 (orange) vs *cry-null* (grey) groups. (G) Bar charts of the average survival percentage at days 1, 3, 5, and 7 in LL of DmCRY vs AgCRY1 (purple) vs *cry-null* groups. (H) Line plot summary of LL survivability of both AeCRY1 and AgCRY1 groups compared with DmCRY and *cry-null*. Data are represented as mean ± SEM. *$p \leq 0.05$, **$p \leq 0.005$, ***$p \leq 0.001$.

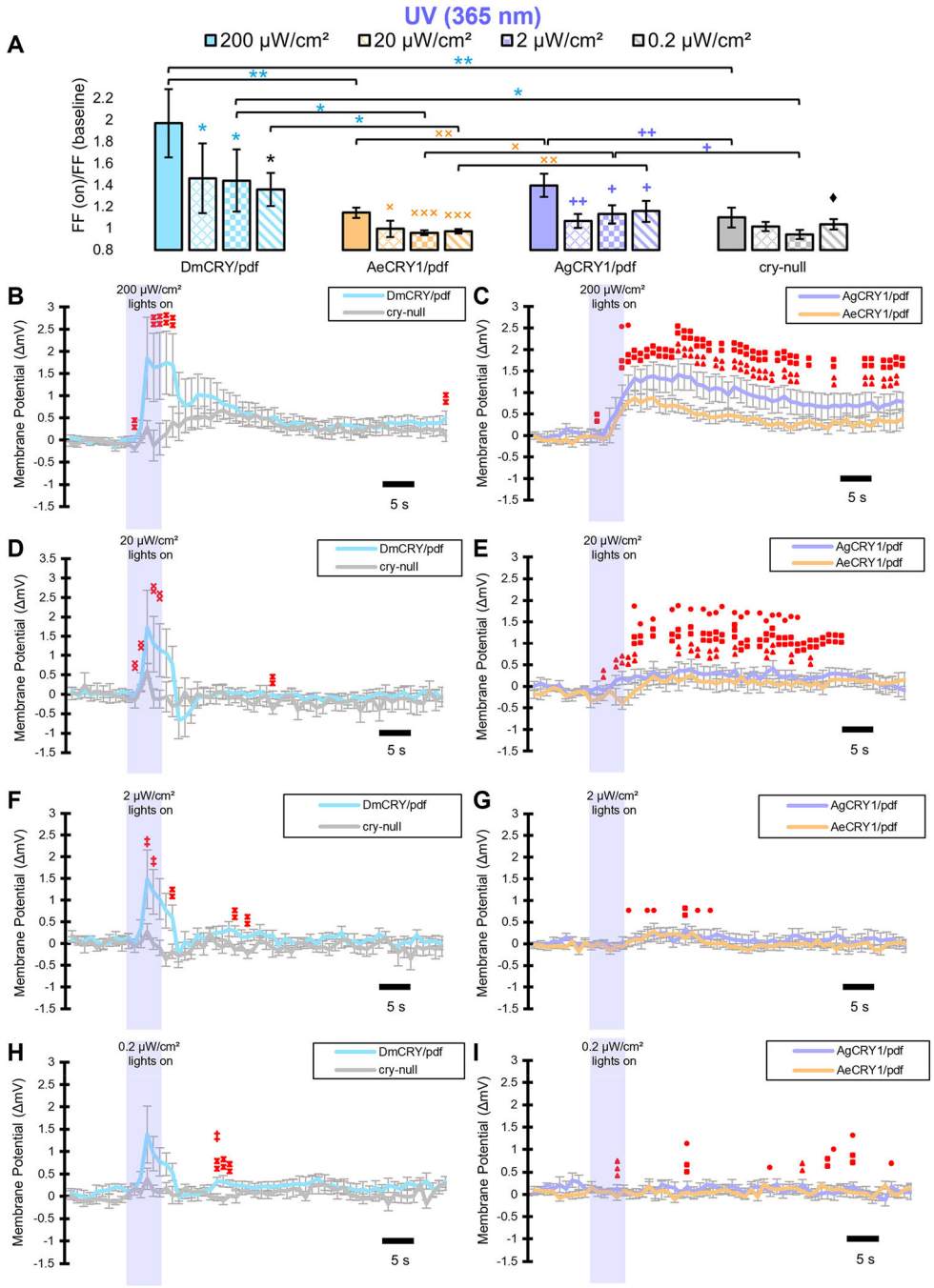

Figure 4. Transgenic PDF+ *Drosophila* Neurons Expressing either AeCRY1 or AgCRY1 Show Intensity-Dependent Light-Evoked Excitation to UV Light

(A) *pdfGAL4* driven DmCRY (light blue) and *cry-null* (grey) comparison of AeCRY1 (light orange) and AgCRY1 (light purple) expressing l-LNvs FF upon five seconds of UV (365 nm) light exposure over 50 seconds of baseline FF at varying intensities light intensities of 200 (solid color), 20 (crisscrossed pattern), 2 (checkered pattern), and 0.2 (diagonally striped pattern) µW/cm^2. Black * indicates $p \leq 0.05$ for comparisons against DmCRY/pdf. Black ♦ indicates $p \leq 0.05$ for comparisons against *cry-null*. Light blue * indicates FDR adjusted $p \leq 0.1$ for comparisons against DmCRY/pdf. Light orange ×

indicates FDR adjusted $p \leq 0.1$ for comparisons against AeCRY1/pdf. Light purple + indicates FDR adjusted $p \leq 0.1$ for comparisons against AgCRY1/pdf. (B-I) Light-evoked change in membrane potential at: 200 $\mu W/cm^2$ UV stimulus for (B) DmCRY (light blue, n=9) vs *cry-null* (grey, n=6) and (C) AeCRY1 (light orange, n=10) vs AgCRY1 (light purple, n=9); 20 $\mu W/cm^2$ UV stimulus for (D) DmCRY (n=8) vs *cry-null* (n=6) and (E) AeCRY1 (n=10) vs AgCRY1 (n=9); 2 $\mu W/cm^2$ UV stimulus for (F) DmCRY (n=8) vs *cry-null* (n=6) and (G) AeCRY1 (n=10) vs AgCRY1 (n=8); and 0.2 $\mu W/cm^2$ UV stimulus for (H) DmCRY (n=8) vs *cry-null* (n=5) and (I) AeCRY1 (n=10) vs AgCRY1 (n=8). Purple bar on membrane potential plots indicates the timing of the 5 seconds of UV-light stimuli and black scale-bar indicates 5 seconds. Traces represent the average last 60 seconds of each recording. Red * indicates FDR adjusted $p \leq 0.1$ between DmCRY/pdf and *cry-null*. Red × indicates FDR adjusted $p \leq 0.1$ between AeCRY1/pdf and DmCRY/pdf. Red + indicates FDR adjusted $p \leq 0.1$ between AgCRY1/pdf and DmCRY/pdf. Red ▲ indicates FDR adjusted $p \leq 0.1$ between AgCRY1/pdf and AeCRY1/pdf. Red ■ indicates FDR adjusted $p \leq 0.1$ between AgCRY1/pdf and *cry-null*. Red ● indicates FDR adjusted $p \leq 0.1$ between AeCRY1/pdf and *cry-null*. Data are represented as mean ± SEM. For black significance symbols: One symbol; $p \leq 0.05$, two symbols; $p \leq 0.005$, three symbols; $p \leq 0.001$. For colored significance symbols: One symbol; $p \leq 0.1$, two symbols; $p \leq 0.05$, three symbols; $p \leq 0.01$. See also Figure S5.

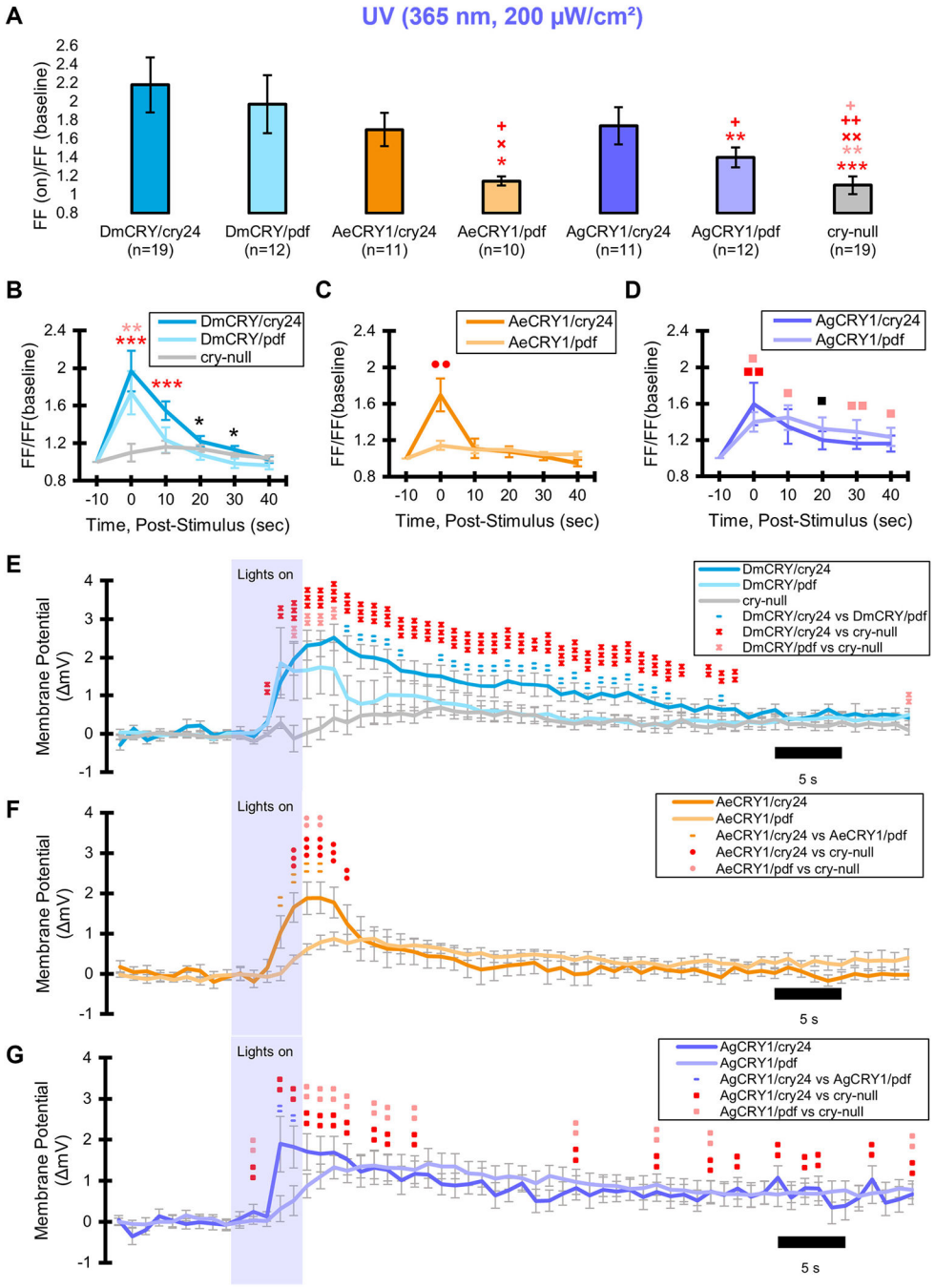

Figure 5. AeCRY1 and AgCRY1 mediate electrophysiological responses to short-wavelength UV light

Light-evoked (A) FF ratio, (B-D) post-stimulus FF, and (E-G) membrane potential responses to UV light stimulus (5 seconds, 365 nm, 200 µW/cm^2) of l-LNvs expressing: (A, B, E) DmCRY (blue, *crypGAL4–24* (n=19); light blue, *pdfGAL4* (n=12); grey, *cry-null* (n=19)), (A, C, F) AeCRY1 (orange, *crypGAL4–24* (n=11); light orange, *pdfGAL4* (n=10)), and (A, D, G) AgCRY1 (purple, *crypGAL4–24* (n=8); light purple, *pdfGAL4* (n=9)) driven by *crypGAL4–24* versus *pdfGAL4* drivers over a *cry-null* background. (E-G) Purple bar on membrane potential plots indicates the timing of the 5 seconds of UV-light stimuli and

black scale-bar indicates 5 seconds. Traces represent the average last 60 seconds of each recording. (A) Red * indicates FDR adjusted $p \leq 0.1$ compared to DmCRY/cry24. Red × indicates FDR adjusted $p \leq 0.1$ compared against AeCRY1/cry24. Red + indicates FDR adjusted $p \leq 0.1$ compared to AgCRY1/cry24. Light red * indicates FDR adjusted $p \leq 0.1$ compared to DmCRY/pdf. Light red + indicates FDR adjusted $p \leq 0.1$ compared to AgCRY1/pdf. (B-G): Black * indicates $p \leq 0.05$ between DmCRY/cry24 and *cry-null*. Black ■ indicates $p \leq 0.05$ between AgCRY1/cry24 and *cry-null*. Red * indicates FDR adjusted $p \leq 0.1$ between DmCRY/cry24 and *cry-null*. Red ■ indicates FDR adjusted $p \leq 0.1$ between AgCRY1/cry24 and *cry-null*. Red ● indicates FDR adjusted $p \leq 0.1$ between AeCRY1/cry24 and *cry-null*. Light red * indicates FDR adjusted $p \leq 0.1$ between DmCRY/pdf and *cry-null*. Light red ■ indicates FDR adjusted $p \leq 0.1$ between AgCRY1/pdf and *cry-null*. Light red ● indicates FDR adjusted $p \leq 0.1$ between AeCRY1/pdf and *cry-null*. Blue − indicates FDR adjusted $p \leq 0.1$ between DmCRY/cry24 and DmCRY/pdf. Orange − indicates FDR adjusted $p \leq 0.1$ between AeCRY1/cry24 and AeCRY1/pdf. Purple − indicates FDR adjusted $p \leq 0.1$ between AgCRY1/cry24 and AgCRY1/pdf. Data are represented as mean ± SEM. For black significance symbols: One symbol; $p \leq 0.05$, two symbols; $p \leq 0.005$, three symbols; $p \leq 0.001$. For colored significance symbols: One symbol; $p \leq 0.1$, two symbols; $p \leq 0.05$, three symbols; $p \leq 0.01$. See also Figures S4, S5, and S6.

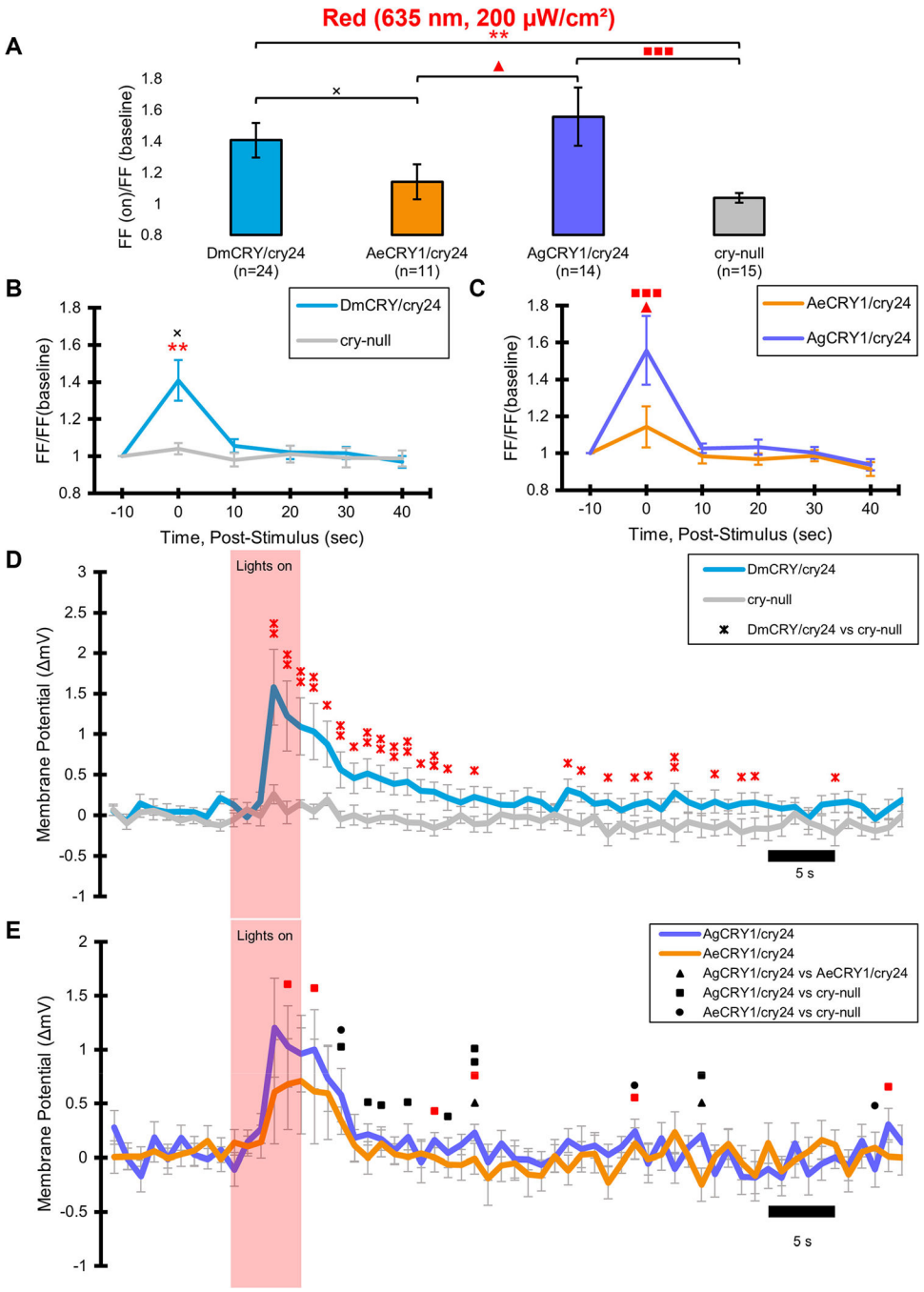

Figure 6. AgCRY1 elicits a strong and robust red-light response, while AeCRY1 does not

Light-evoked (A) FF ratio, (B, C) post-stimulus FF, and (D, E) membrane potential comparison of red-light (635 nm, 200 µW/cm^2) excited l-LNvs expressing: (A, B, D) DmCRY (blue, n=24) and negative control *cry-null* (grey, n=15), (A, C, E) AeCRY1 (orange, n=11) and AgCRY1 (purple, n=14). (D, E) Red bar on membrane potential plots indicates the timing of the 5 seconds of red-light stimuli and black scale-bar indicates 5 seconds. Traces represent the average last 60 seconds of each recording. (A-E) Black × indicates $p \leq 0.05$ between AeCRY1/cry24 and DmCRY/cry24. Black ▲ indicates $p \leq 0.05$

between AgCRY1/cry24 and AeCRY1/cry24. Black ■ indicates $p \leq 0.05$ between AgCRY1/cry24 and *cry-null*. Black ● indicates $p \leq 0.05$ between AeCRY1/cry24 and *cry-null*. Red * indicates FDR adjusted $p \leq 0.1$ between DmCRY/cry24 and *cry-null*. Red ▲ indicates FDR adjusted $p \leq 0.1$ between AgCRY1/cry24 and AeCRY1/cry24. Red ■ indicates FDR adjusted $p \leq 0.1$ between AgCRY1/cry24 and *cry-null*. Data are represented as mean ± SEM. For black significance symbols: One symbol; $p \leq 0.05$, two symbols; $p \leq 0.005$, three symbols; $p \leq 0.001$. For colored significance symbols: One symbol; $p \leq 0.1$, two symbols; $p \leq 0.05$, three symbols; $p \leq 0.01$. See also Figure S7.

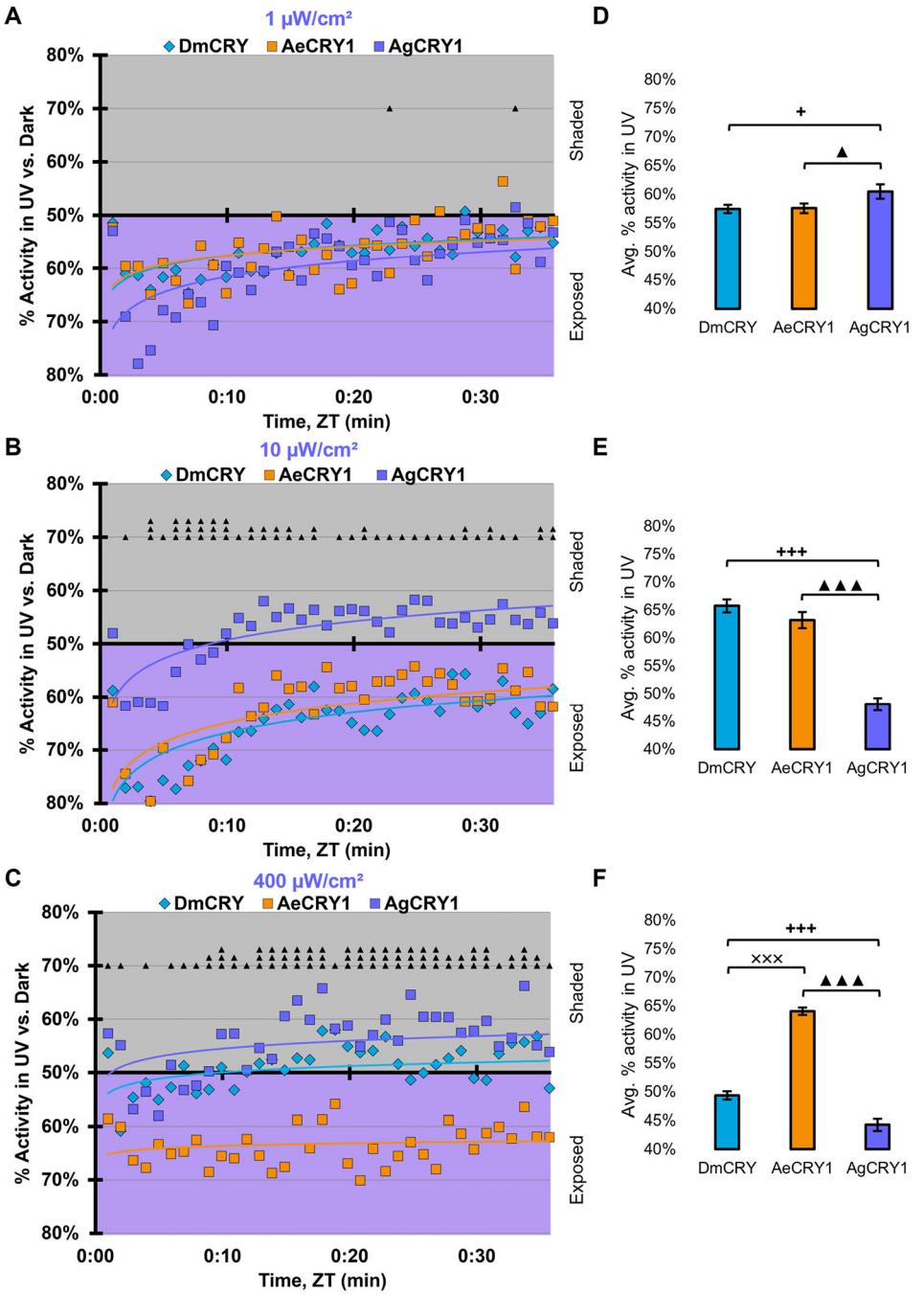

Figure 7. Mosquito CRY1s confer species-specific and intensity-dependent behavioral attraction and avoidance to UV light

(A-C) UV attraction/avoidance behavior is measured by % activity in a dark shaded environment versus (A) very low-intensity (1 µW/cm^2), (B) moderately low-intensity (10 µW/cm^2), and (C) high-intensity (400 µW/cm^2) UV-exposed environments (365 nm) during the light phase of a standard 12:12 hr LD cycle. Preference is calculated by percentage of activity in each environment over total activity for each time bin. (A) DmCRY (blue, n=76) vs. diurnal AeCRY1 (orange, n=65) vs. nocturnal AgCRY1 (purple, n=65) expressing flies show a strong attraction to very low-intensity (1 µW/cm^2) UV light in the first 30 minutes of

UV light exposure. (B) Daytime-active DmCRY (blue, n=76) and AeCRY1 (orange, n=76) flies show a maintained, slightly stronger attraction to low-intensity (10 μW/cm^2) UV light in the first 30 minutes of UV light exposure, whereas nocturnal AgCRY1 (purple, n=78) expressing flies show a fast, strong negative phototaxis after a few minutes of UV light exposure. (C) DmCRY (blue, n=73) and AgCRY1 (purple, n=72) expressing flies show a strong and very fast negative phototaxis to high-intensity (400 μW/cm^2) UV light in the first couple minutes of UV light exposure, whereas diurnal AeCRY1 (orange, n=63) remain strongly attracted to the UV environment. All plots are shown from ZT 0–30 min in 1-min bins. (D-F) Quantified mean % activity of flies in UV environment across the first 30 minutes for (D) very low-intensity, (E) moderately low-intensity, and (F) high-intensity UV light environments. Black + indicates $p \leq 0.05$ between AgCRY1/cry24 and DmCRY/cry24. Black × indicates $p \leq 0.05$ between AeCRY1/cry24 and DmCRY/cry24. Black ▲ indicates $p \leq 0.05$ between AgCRY1/cry24 and AeCRY1/cry24. Data are represented as mean ± SEM. One significance symbol; $p \leq 0.05$, two significance symbols; $p \leq 0.005$, three significance symbols; $p \leq 0.001$.

KEY RESOURCES TABLE

REAGENT or RESOURCE	SOURCE	IDENTIFIER
Antibodies		
Goat anti-mouse Alexa Fluor 488	Invitrogen	Cat# A-11001; RRID: AB_2534069
Goat anti-rabbit Alexa Fluor 594	Invitrogen	Cat# A-11037; RRID: AB_2534095
Rabbit anti-TIM, polyclonal	Amita Seghal, University of Pennsylvania	N/A
Chemicals, peptides, and recombinant proteins		
Paraformaldehyde	Alfa Aesar/Fisher Scientific	Cat# AA433689L
Triton-X	Fisher Scientific	Cat# T8787
PBS	VWR International	Cat# 12001-766
Horse Serum	Fisher Scientific	Cat# MT35030CV
Glycerol	Fisher Scientific	Cat# G33-500
Kgluconate	Alfa Aesar/Fisher Scientific	Cat# B2513518
NaCl	Alfa Aesar/Fisher Scientific	Cat# S271-500
CaCl2	Alfa Aesar/Fisher Scientific	Cat# L1319130
MgCl2-6H2O	Alfa Aesar/Fisher Scientific	Cat# NC0944617
HEPES	Alfa Aesar/Fisher Scientific	Cat# 61034RO
EGTA	RPI	Cat# E57060
KCl	Alfa Aesar/Fisher Scientific	Cat# 2210914
MgCl2	Alfa Aesar/Fisher Scientific	Cat# 3570709
Glucose	Alfa Aesar/Fisher Scientific	Cat# 388190010
Deposited data		
Raw and analyzed data	This paper	
Experimental models: Organisms/strains		
Drosophila (*crypGAL4-24*; *UAS-DmCRY-eGFP; cry01*)	[20]	N/A
Drosophila (*crypGAL4-24*; *UAS-AeCRY1-eGFP; cry01*)	This paper	N/A
Drosophila (*crypGAL4-24*; *UAS-AgCRY1-eGFP*; *cry01*)	This paper	N/A
Drosophila (*pdfGAL4*; *UAS-AeCRY1-eGFP*; *cry01*)	This paper	N/A
Drosophila (*pdfGAL4*; *UAS-AgCRY1-eGFP*; *cry01*)	This paper	N/A
Drosophila (w1118;+; *cry01*)	Jeff Hall, Brandeis University	RRID:BDSC_86267
Oligonucleotides		
Primer: AeCRY1 Forward: CGA GAA AGT GCA GGC CAA CAA TC Reverse: GT TCT TCA ACT CCG GCA GAT ATC	This paper	N/A

REAGENT or RESOURCE	SOURCE	IDENTIFIER
Primer: AgCRY1 Forward: CAG CCA GTT CAA GTA TCC GG Reverse: CGG TTC GTG CAC AAA CTG TG	This paper	N/A
Recombinant DNA		
XhoI-eGFP-LoxP-linkers-AgCry1-CDS-XbaI 2,428	Genscript	N/A
XhoI-eGFP-LoxP-linkers-AeCry1-CDS-XbaI_pJFRC7	Genscript	N/A
Software and algorithms		
ImageJ	Fiji	https://imagej.nih.gov/ij/
MATLAB	Mathworks	https://www.mathworks.com/products/matlab.html
Microsoft Excel	Microsoft	https://www.microsoft.com/en-us/microsoft-365/microsoft-office
Minitab Statistical Software	Minitab	https://www.minitab.com/en-us/
Axon pCLAMP 10.3.2.1/Clampfit 10.7.0	Molecular Devices	https://support.moleculardevices.com/s/article/Axon-pCLAMP-10-Electrophysiology-Data-Acquisition-Analysis-Software-Download-Page
DAMSystem311/DAMFileScan113	Trikinetics	https://www.trikinetics.com/
FaasX	NeuroPSI	https://neuropsi.cnrs.fr/en/departments/cnn/group-leader-francois-rouyer/
ClockLab	ActiMetrics	https://actimetrics.com/products/clocklab/
Other		
Pyrex glass tubes	Trikinetics	Cat# PGT25×125
Locomotor Activity Monitors	Trikinetics	N/A
UV light	Philips	Cat# TL-D/08
Light Meter	Newport	Cat# 843-R
Light Sensor	Newport	Cat# 818-UV
Neutral Density Filters	GamColor CineFilter	Cat# CL211
Incubators	Percival Scientific	Cat# DR-36VL
Micromanipulator	WPI	MP-225
Axon Digidata 1322A	Axon Instruments	1322A
Leica SP8 UV/Visible Laster Confocal	Leica	TCS SP8
Quickchange II	Agilent	Cat# 200523